Density Functional Theory Study of Spirodienone Stereoisomers in Lignin

Thomas Elder*†, Laura Berstis‡§, Gregg T. Beckham‡, Michael F. Crowley‡§

† USDA-Forest Service, Southern Research Station, 521 Devall Dr., Auburn, AL 36849
‡ National Bioenergy Center, National Renewable Energy Laboratory, 15013 Denver W Pkwy, Golden, CO 80401
§Biosciences Center, National Renewable Energy Laboratory, 15013 Denver W Pkwy, Golden, CO 80401

*telder@fs.fed.us 334-826-8700 x 148

Abstract

The spirodienone structure in lignin is a relatively recent discovery, and has been found to occur in lignin of various plant species at concentrations of ~3% which is sufficiently high to be important for better understanding of its properties and reactivity. The cyclic structure, with a β-1 bond has been proposed to be a precursor for acyclic β-1 linkages in lignin. Previous analytical work has revealed the presence, but not the absolute configuration, of two stereoisomeric forms of spirodienone. The objective of the current work was to determine if there are thermodynamic differences that could help identify the experimentally observed stereoisomers. Results from density functional theory calculations reveal the presence of clusters of stereoisomers with varying stability that may be of use in narrowing the list of possible structures. Furthermore, the bond dissociation enthalpy of the cyclic ring exhibited a particularly high value for the C-O cleavage reaction relative to more conventional ether bonds in lignin, perhaps due to limited electron delocalization possibilities.

Keywords

lignin, spirodienone, density functional theory, stereoisomerism, bond dissociation energy

Introduction

The general structure of lignin generated from the polymerization of the cinnamyl alcohols (coniferyl, sinapyl, and *p*-coumaryl alcohol) has been the topic of intense scrutiny and extensive literature attention.[1] As such, the more familiar interunit linkages (e.g. β-O-4, phenylcoumaran, pinoresinol, 5-5') are well known. More recently, however, additional lignin linkages have been found, such as dibenzodioxocin[2-4] and the homopolymeric catechol lignins that polymerize linearly through benzodioxane units.[5-7] The current work addresses another such linkage, the spirodienone trimer (Figure 1) that was first reported by Zhang and Gellerstedt.[8] Working with spruce and aspen, they found spirodienone structures at levels of 3 and 1.8% respectively. In subsequent work, spruce and birch were found to contain 3% spirodienone, and 4% in kenaf, with guaiacyl spirodienones in spruce and syringyl spirodienones in birch and kenaf.[9] Following these initial identifications, spirodienone structures have been detected in bamboo[10, 11], eucalyptus[12-15], and cottonwood[16,17], at levels of ~6-8%, 1-5% and 1%, respectively. While somewhat low, these values are similar to those of some of the other minor linkages, such as the phenylcoumarans and pinoresinols. It can be seen that the spirodienone trimer is stereochemically complex, although in fresh spruce only two stereoisomers were detected, while in aged spruce, 1 stereoisomer was found.[8] In later work on freshly cut spruce, birch, and kenaf, two stereoisomers were found, one of which was present in higher levels.[9] These results notwithstanding, to date the absolute configuration of the spirodienone structure(s) in lignin have not been reported. In the absence of definitive stereochemical assignments, the objective of the current work is to determine, by the application of density functional theory (DFT) calculations, if thermodynamic stability varies with stereochemistry and the configuration of the more stable stereoisomers. The calculated relative stability of the spirodienones indicate which of the

3

stereoisomers are thermodynamically preferred, and potentially predict the stereochemical

composition of natural lignin polymers. The formation of spirodienones is proposed to occur

through coupling of monolignol and β-O-4' end-group radicals, to give a dienone/quinone

methide intermediate, which undergoes ring closure, resulting in the spirodienone.[9] Given this

two-step process, there are several points at which both kinetics and thermodynamics could

influence the stereochemistry of the products. While recognizing the importance of these

reactions and the possible role of kinetics in the formation of the spirodienones, the present work

is focused solely on the relative thermodynamics of the products. Lastly, lignin is well-known

to undergo complex reactions during mechanical, chemical, and thermal treatments that are key

to biomass conversion processes and lignin valorization efforts. Given the abundance of

spirodienones in lignin, their behavior in ring-opening reactions is also addressed Computational

evaluation of bond dissociation enthalpies (BDE) in other cyclic lignin models, including

phenylcoumaran[18], dibenzodioxocin[19], pinoresinol[20], and the catechol lignols[21,22], have improved

our understanding of bond strengths, and the ensuing potential impacts on polymerization and

depolymerization. The spirodienone structure itself has also been the subject of recent

computational work, applying steered *ab initio* molecular dynamics to bond cleavage reactions,

such as potentially could occur from mechanochemical or sonochemical treatments.[23]

Methods

The structure of guaiacyl spirodienones, shown in Figure 1, includes 5 chiral carbons, generating

the possibility of 32 stereoisomers or 16 enantiomeric pairs. In previous work,[21,22] it was found

that the enthalpies calculated for enantiomers were generally within "chemical accuracy".[24]

4

Given this level of agreement, for the current work, sixteen stereoisomers are identified, representing one member of each enantiomeric pair, as shown in Figure 2.

A two-step conformational search was performed for each stereoisomer, wherein a Monte Carlo search with 1,000 iterations and force-field minimization using MMFF, was followed by PM6 optimization as implemented in Spartan'16.[25] The 10 lowest energy conformations from the PM6 optimizations were subsequently optimized with M06-2X/6-31+G(d), using the default criteria of 0.00045 hartrees/bohr, 0.0003 hartrees/bohr, 0.0018 bohr and 0.0012 bohr for maximum force, root mean square force, maximum displacement and root mean square displacement, respectively and the ultrafine integration grid consisting of 99 radial shells and 590 angular points per shell. The lowest energy conformation from this step was further optimized and refined with M06-2X/6-311++G(d,p), again with the ultrafine integration grid and default optimization criteria. Frequency calculations were performed at 298.15 K to ensure the identification of a local minimum geometry, and to obtain thermal corrections for enthalpy evaluations. The DFT calculations were executed with Gaussian09[26] and Gaussian16[27], using the resources of the Texas Advanced Computer Center, the Pittsburgh Supercomputing Center, and the Alabama Supercomputer Authority.

Based on the lowest energy stereoisomer, BDEs were calculated as previously described for the ring-opening and cleavage reaction products shown in Figure 3. The ring-opened products were modelled as triplets in accordance with the results reported by Younker[18], and as reported in the earlier literature[21,22], the salient bonds were deleted and the interatomic distance was increased to 2.5 Å in order to examine a nearby minimum and prevent recombination during optimization.

5

Results and Discussion

The relative enthalpies of the stereoisomers calculated at the M06-2X/6-311++G(d,p) level and 298.15 K are shown in Figure 4. The most stable stereoisomer is **6** with RRSRS stereochemistry, followed by **11** (RSRSR) which is 1.32 kcal mol^{-1} less stable, which falls within the range of ±2.0 kcal mol^{-1}, set for "chemical accuracy" of DFT calculations.[24] As such, the energy difference between these stereoisomers would be indistinguishable. More recently, however, there has been a tendency to reduce this value to 1 kcal mol^{-1},[28] and errors of 0.75 kcal mol^{-1} have been reported for DFT calculations.[29] Based on the latter arguments, structures **6** and **11** may potentially be defined as energetically separable. Assuming a difference of 1.32 kcal mol^{-1} as a threshold, several clusters of stability can be seen in the Figure 4, in which the points enclosed by the same color ellipse differ by less than this level. The group **11**, **15**, **16**, **12**, **14** (in order of stability) cover a range of 0.90 kcal mol^{-1}, and are distinct from all others. The less stable stereoisomers (**8**, **13**, **9**, **10**, **3**, **1**, **5**, **4**, **7**, **2**, in order of stability) span a range of 2.68 kcal mol^{-1}, but with some degree of overlap, especially among **8**, **13**, **9**, and **10**. The least stable stereoisomers (**10** through **2**) with a range of 1.28 kcal mol^{-1}, are between 3.7 and 6.2 kcal mol^{-1} less stable than isomer **6**. In addition, the six stereoisomers with the highest energies all exhibit the β-R configuration. The results from these calculations specifically address the stated objectives, demonstrating that stability of the spirodienone trimer does indeed vary with stereochemistry and that there are populations of low lying stereoisomers that would be thermodynamically preferred.

6

Subsequent to this examination of relative enthalpies, results for Gibbs free energy, at 298.15 K, were extracted. The range of these values is smaller, at 4.8 kcal mol^{-1}, as opposed to 6.2 kcal mol^{-1} for the enthalpies. As such, and assuming the previously established 1.32 kcal mol^{-1}, as the criterion for separation, there is considerably more overlap between the clusters of stereoisomers. Furthermore, while there are differences in ordering, the results for Gibbs free energy are qualitatively similar to the enthalpies, with stereoisomers **6** and **11** in the lowest energy population.

The geometries for these structures are shown in Figure 5. From Figure 5, it can be seen that structure **6** has an interesting conformation in which the B and C rings of the spirodienone adopt a displaced sandwich arrangement, similar to that described for aromatic dimers.[30] In addition, the orbital plots (Figure 6) show a concentration of HOMO density on the C-ring and LUMO density on the B-ring. Such a conformation and orbital populations may account for the relative stability of this structure.

Given the assumption that **6** is energetically distinct and that there have been reports of spirodienone existing in two stereoisomeric forms, an examination of the next group of structures is in order. These are (in order of stability) **11**, **15**, **16**, **12**, and **14**, with a range in enthalpy of 0.89 kcal mol^{-1}, which would mean that their separation based on stability is tenuous. It may be worth noting, however, that all of these structures are in the β-S configuration, while **6** is β-R. Among these stereoisomers, **11** and **12** exhibit similar parallel arrangements of the B- and C-rings as also exhibited by **6**, and differ only by inversion about the C-1 position. Structure **14** has

a similar conformation, but with some twisting of the C-ring. Stereoisomers **15** and **16** also differ from each other only in configuration at C-1, but have a non-parallel conformation between the B- and C-rings. An examination of the frontier molecular orbitals (Figure 6) of these lower energy stereoisomers reveals that for structures **6** and **14**, the HOMO is concentrated on the C-ring, while the LUMO is confined to the B-ring. In contrast, for **11**, **15**, **16**, and **12** the HOMO density is on the A-ring, while the LUMO density remains on the B-ring. Given that structures **11**, **15**, **16**, **12**, and **14** cannot be definitively separated based on stability, the similarity in orbital densities between **6**, arguably the most stable stereoisomer, and **14** might be indicative of the two stereoisomers that have been identified by NMR.[8,9] While these differences are not sufficient to conclusively identify thermodynamic preferences, the relative stability of these stereoisomers may be of use in narrowing the list of possible structures. Further, the lack of any two distinctly most thermodynamically stable isomers may point to the kinetics of polymerization as responsible for the experimentally observed, but as yet unassigned spirodienone stereoisomers.

Based on the results for structure **6**, the most stable stereoisomer, the BDEs for the radical products in Figure 3 are presented in Table 1. Products **3** and **4**, involving C-C bond cleavage, have the lowest BDE values (45.50-50.52 kcal mol^{-1}). Products **1**, **2**, and **5** (71.92-89.15 kcal mol^{-1}) are markedly higher, even though **1** and **5** result from C-O bond breaking. Previous work on cyclic linkages of lignin have shown that for phenylcoumarans, the C-C and C-O bonds have BDEs of ~60 and 40 kcal mol^{-1}, respectively.[18] Within the dibenzodioxocin ring[19], C-O bonds are in the 45-57 kcal mol^{-1} range, while the BDE for the aliphatic carbons are ~72 kcal mol^{-1}. In pinoresinols[20], the aliphatic C-C bonds vary from ~66-80 kcal mol^{-1}, and the C-O bonds ~68-78

kcal mol^{-1}. For further comparison, the C-O bonds in catechol lignin[21,22] dimers exhibit a range

of BDEs of 50-60 kcal mol^{-1}. The particularly high BDE values associated with C-O bond

cleavage in the current work may be accounted for by the presence of tertiary carbon radical

centers in **3** and **4**, while **1**, **2**, and **5** contain secondary carbon radicals and oxygen radicals, both

of which are factors that contribute to decreased radical stability. Furthermore, the interruption

of the trimeric system by the aliphatic B-ring limits delocalization of the unpaired electrons in

the triplet products. It can also be seen that ring B of radicals **3** and **4** would have more aromatic

character than **1**, **2**, and **5**, as evidenced by the bond lengths (Table S26). Perhaps more

importantly however, the current results are consistent with those from work done on

spirodienone with *ab initio* molecular dynamics[23] in which energies of ring opening products **3**

and **1**, were ~43 and 120 kcal mol^{-1}, respectively. While the latter value is higher than calculated

in the current work, this independent observation also shows that the BDE for C-O cleavage in

spirodienone is higher than C-C bond breaking. The doublet products, **6a-6b** and **7a-7b**,

resulting from C-C and C-O cleavages, with bond dissociation energies of 90.97 and 72.02 kcal

mol^{-1}, respectively, are qualitatively similar to the values of 84.71 and 51.42 kcal mol^{-1} from *ab*

initio molecular dynamics.[23] Lastly, given the size and complex ring structure of these models,

the importance of non-covalent interactions could be proposed. While density functional

methods are known to be problematic where dispersion forces are concerned, the M06-2X

functional has been reported to perform very well in this regard.[31-33]

It may be interesting to note that genetic manipulation of both softwoods[34] and hardwoods[35] have

resulted in lignins with elevated levels of spirodienone structures. Based on the low BDEs

associated with the aforementioned B-ring of the system, it is conceivable that such alterations might be reflected in the overall reactivity of the engineered lignins.

Conclusions

The spirodienone structure in lignin is a relatively recent discovery, which depending on the plant species, occurs at levels of ~3%, similar to that of pinoresinol and dibenzodioxocin. Furthermore, genetic manipulations have resulted in elevated levels of spirodienone. As such, its presence should not be neglected in the ongoing efforts to understand the properties of lignin. The reactivity of spirodienone linkages may influence the behavior of the polymer, and affect depolymerization chemistry. In the initial reports on spirodienone, spectroscopic evidence indicated that one or sometimes two stereoisomers were present. Given this experimental result and the chiral complexity of the structure, the current work examined the stereoisomers representing one set of enantiomers to determine if there is a thermodynamic preference as a function of stereochemistry. The relative enthalpies of all 16 stereoisomers span a range of 6.2 kcal mol^{-1}. Among the more stable structures, the RRSRS stereoisomer has the lowest enthalpy, and depending on the definition of "chemical accuracy" adopted may be interpreted as the thermodynamically most stable stereochemical configuration. The geometry of this structure reveals that two of the rings are in a displaced-parallel arrangement, with the density of the frontier molecular orbitals on each of the rings in question, perhaps contributing to its relative stability. Based on these findings, BDEs were determined for the RRSRS stereoisomer as a measure of its reactivity. Among the ring-opening reactions, those involving the quinone ring, which generated tertiary carbon radicals were quite low, while the C-O cleavages were higher

10

than in other lignin models. The higher C-O BDEs may be due to the presence of the quinone that limits electron delocalization opportunities.

Supporting Information

The Supporting Information contains the Cartesian coordinates for the low energy conformation of each stereoisomer and radical product, optimized using the 6-311++G(d,p) basis set, and bond lengths for the B-ring in radical products **1**, **2**, **3**, **4** and **5**.

bond dissociation enthalpy (298 K) kcal mol^{-1}	product
89.15	radical **1**
71.92	radical **2**
45.50	radical **3**
50.52	radical **4**
82.42	radical **5**
90.97	radical **6a+6b**
72.02	radical **7a+7b**

Table 1. Bond dissociation enthalpies of spirodienone **6** (RRSRS).
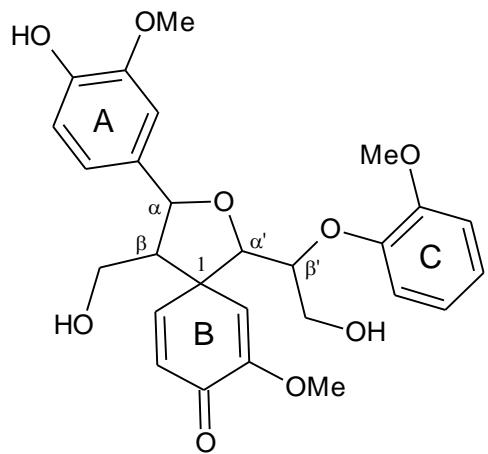
Figure 1. Molecular structure of guaiacyl-spirodienone, with five stereocenters notated as: **α**, **β**, **α'**, **β'** and **1** .
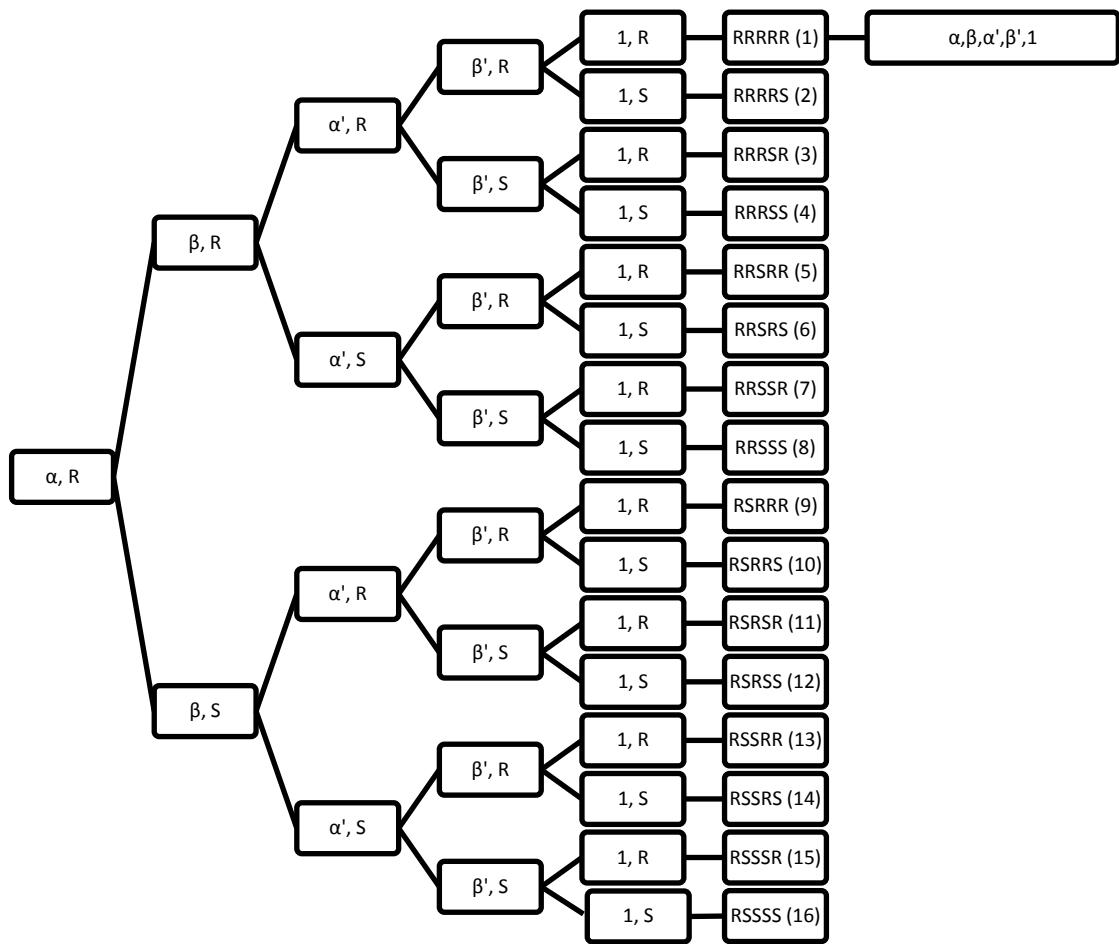
Figure 2. Stereoisomers representing one enantiomer of each pair.
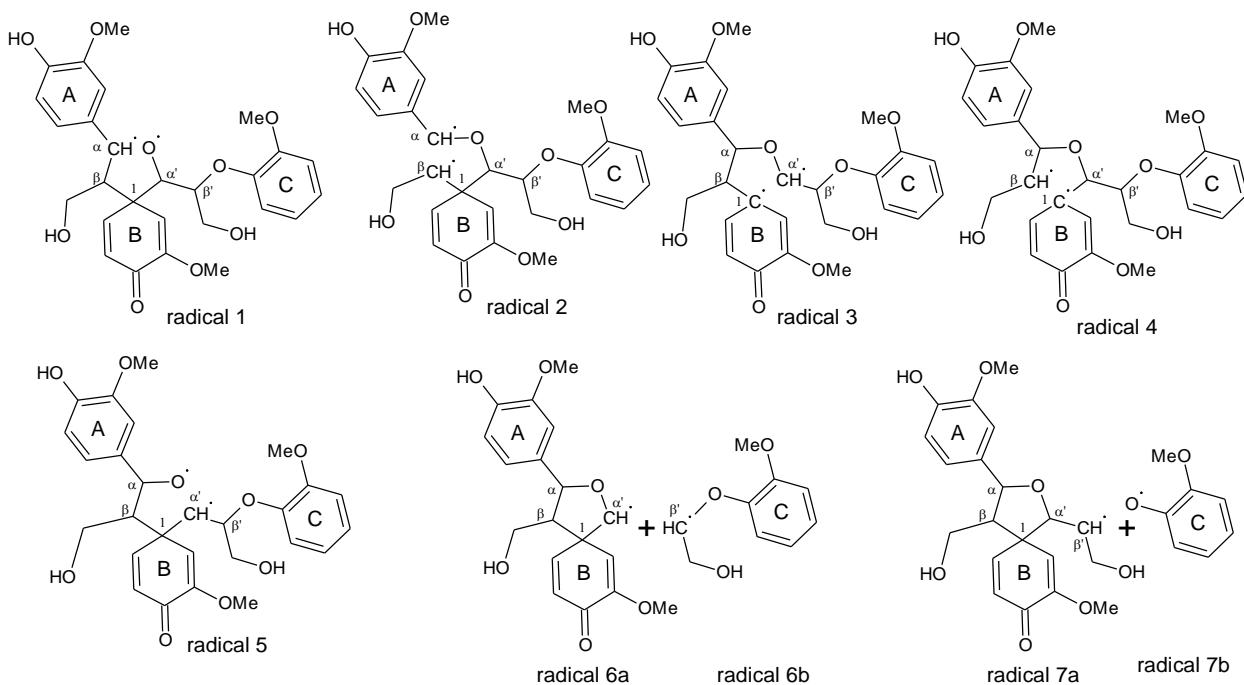
Figure 3. Bond cleavage products of the spirodienone trimer for determination of bond dissociation enthalpies.
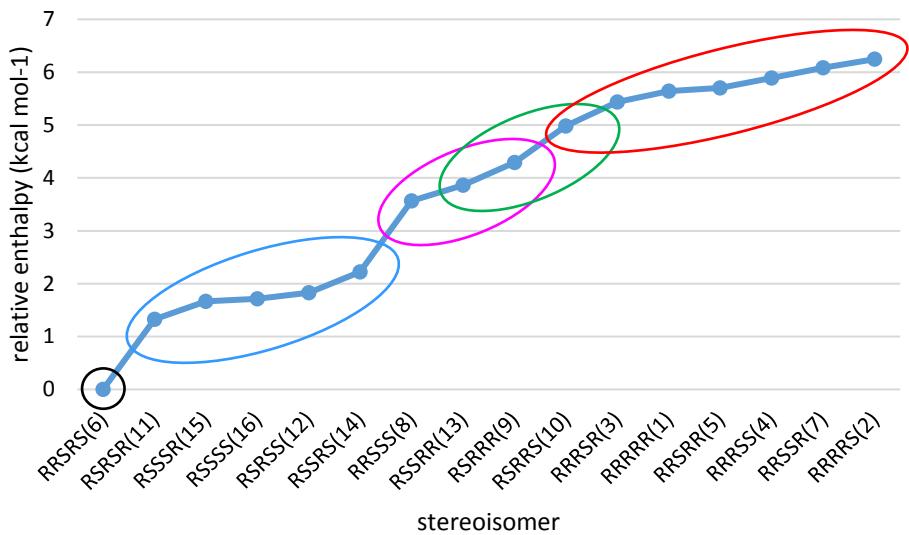
Figure 4. Relative enthalpies of stereoisomers optimized at M06-2X/6-311++G(d,p) level. Stereoisomer designations refer to the number and configurations from Figure 2. Points enclosed by the same color ellipse have enthalpy differences of less than 1.32 kcal mol^{-1}.

1-RRRRR

2-RRRRS

3-RRRSR

4-RRRSS

5--RRSRR

6-RRSRS

7-RRSSR

8-RRSSS

9-RSRRR

10-RSRRS

11-RSRSR

12-RSRSS

13-RSSRR

14-RSSRS

15-RSSSR

16-RSSSS
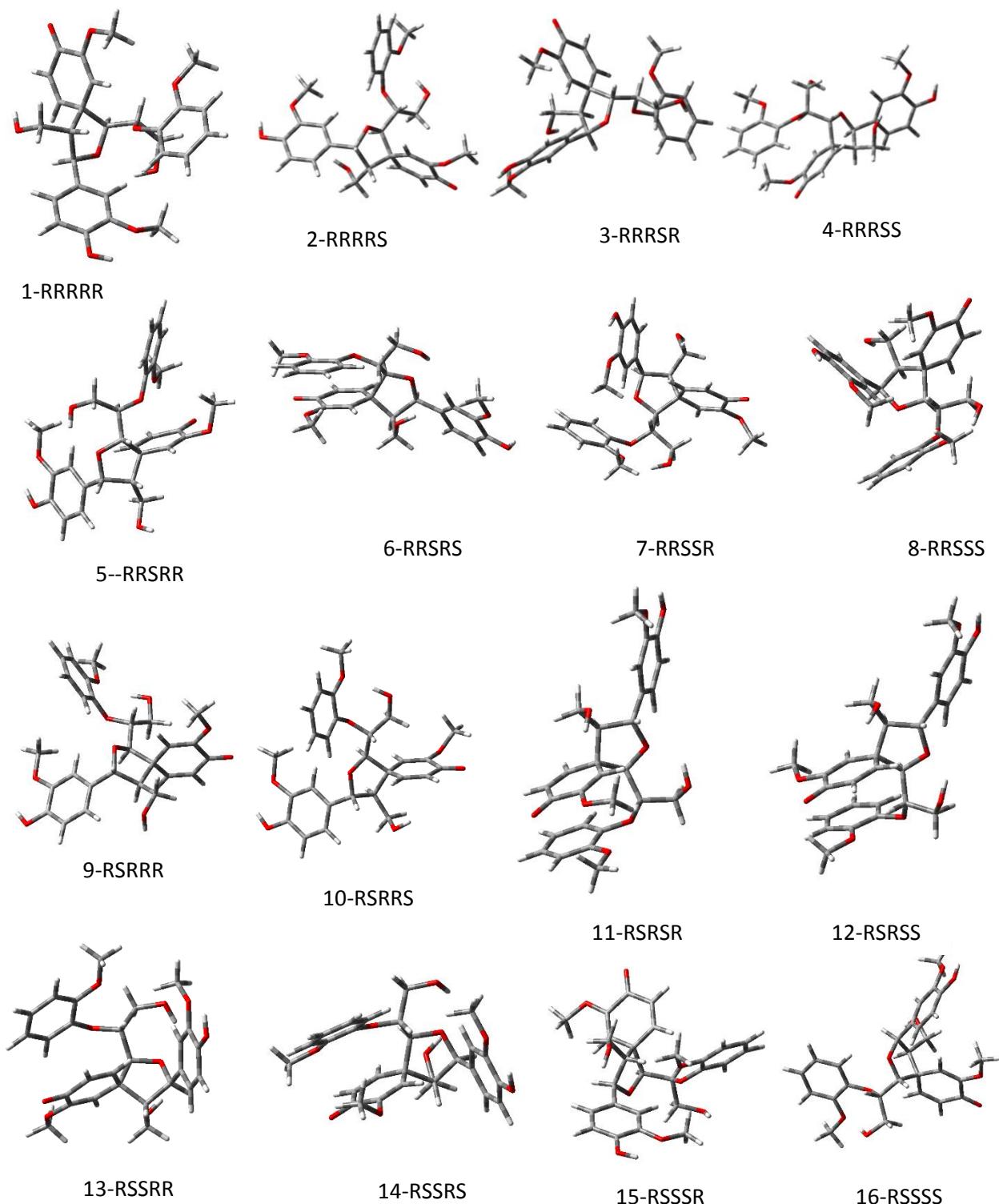
Figure 5. Optimized geometries of stereoisomers.

HOMO   LUMO

6--RRSRS

11-RSRSR

15-RSSSR

16-RSSSS

12-RSRSS

14-RSSRS
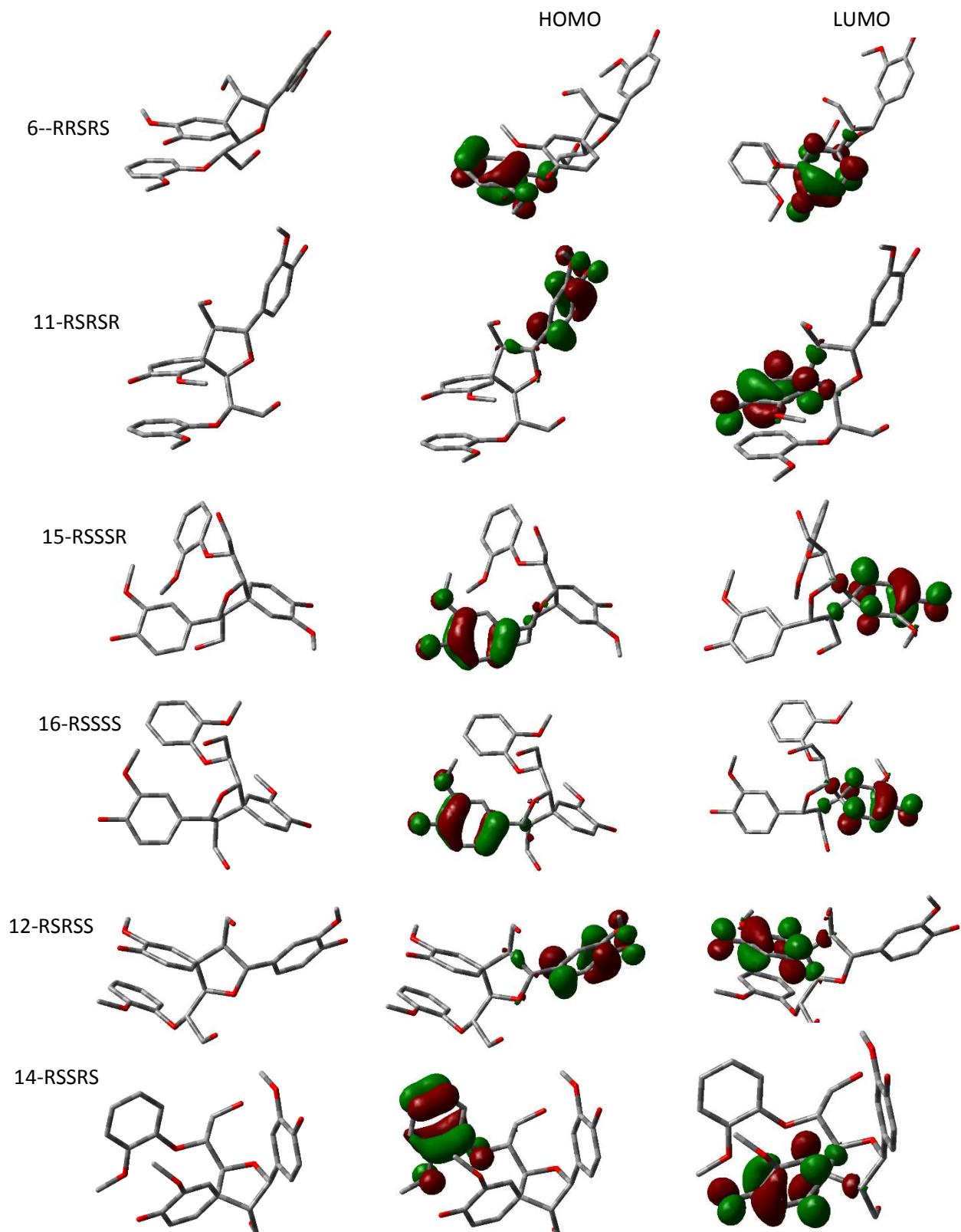
Figure 6. Geometries and plots of HOMO and LUMO density for the more stable stereoisomers.

Table of Contents Graphic

Density Functional Theory Study of Spirodienone Stereoisomers in Lignin

Thomas Elder, Laura Berstis, Gregg T. Beckham, Michael F. Crowley

Optimized geometry and frontier molecular orbitals of the low energy spirodienone stereoisomer in lignin.

Acknowledgements

References

1. Vanholme, Ruben; Demedts, Brecht; Morreel, Kris; Ralph, John; Boerjan, Wout. Lignin Biosynthesis and Structure, *Plant Physiol.* **2010,** *153,* 895-905

2. Karhunen, P.; Rummakko, P.; Sipila, J.; Brunow, G.; Kilpelainen,I. Dibenzodioxocins; a novel type of linkage in softwood lignins *Tetrahedron Lett.* **1995**, *36*, 169−170.

3. Karhunen, P.; Rummakko, P.; Pajunen, A.; Brunow, G. J. *Chem.Soc., Perkins Trans. 1* **1996**, *1996*, 2303−2308.

4. Karhunen, P.; Mikkola, J.; Pajunen, A.; Brunow, G. The behaviour of dibenzodioxocin structures in lignin during alkaline pulping processes, *Nord. PulpPap. Res. J.* **1999**, *14*, 123−128.

5. Chen, F.; Tobimatsu, Y.; Havkin-Frenkel, D.; Dixon, R. A.; Ralph, J. A polymer of caffeyl alcohol in plant seeds, *Proc. Natl. Acad. Sci. U. S. A.* **2012**, *109*, 1772-1777.

6. Chen, F.; Tobimatsu, Y.; Jackson, L.; Nakashima, J.; Ralph, J.; Dixon, R. A. Novel seed coat lignins in the Cactaceae: structure, distribution and implications for the evolution of lignin diversity, *Plant J.* **2013**, *73*, 201-211.

7. Tobimatsu, Y.; Chen, F.; Nakashima, J.; Escamilla-Trevino, L. L.; Jackson, L.; Dixon, R. A.; Ralph, J. Coexistence but independent biosynthesis of catechyl and guaiacyl/syringyl lignin polymers in seed coats, *Plant Cell* **2013**, *25*, 2587-2600.

8. Zhang, L.; Gellerstedt, G. NMR observation of a new lignin structure, a spiro-dienone, *Chem. Commun,* **2012**, 2744-2745.

9. Zhang, L.; Gellerstedt, G; Ralph, J.; Lu, F. NMR studies on the occurrence of spirodienone structures in lignins. *J. Wood Chem. Technol*, **2006**, *26*, 65-79.

10. Huang, C.X.; He, J.; Du, L.T.; Min, D.Y.; Yong, Q. Structural characterization of the lignins from the green and yellow bamboo culm (*Phyllostachys pubescens*). *J. Wood Chem. Technol*, **2016**, *36*, 157-172.

11. Shi, Z.J; Xiao, L.P; Jia-Deng; Xu, F.; Sun, R.C. Physicochemical characterization of lignin fractions sequentially isolated from bamboo (*Dendrocalamus brandisii*) with hot water and alkaline ethanol solution. *J. Appl. Polym. Sci.*, **2012**, *125* , 3290-3301

12. Yanez, M. ; Matsuhiro, B; Nunez, C.; Pan, S.B.; Hubbell, C.A.; Sannigrahi, P.; Ragauskas, A.J. Physicochemical characterization of ethanol organosolv lignin (EOL)

from *Eucalyptus globulus*: Effect of extraction conditions on the molecular structure, *Polym. Degrad. Stab.* **2014**, *110,* 184-194.

13. Rencoret, J. ; Gutierrez, A.; Nieto, L.; Jimenez-Barbero, J.; Faulds, C.B.; Kim, H.; Ralph, J.; Martinez, A.T.; del Rio, J.C. Lignin composition and structure in young versus adult *Eucalyptus globulus* plants, *Plant Physiol.*, **2011**, *155,* 667-682.

14. Rencoret, J.; Marques, G.; Gutierrez, A.; Ibarra, D.; Li, J.; Gellerstedt, G.; Santos, J.I.; Jimenez-Barbero, J.; Martinez, A.T.; del Rio, J.C. Structural characterization of milled wood lignins from different eucalypt species. *Holzforschung*, **2008**, *62,* 514-526.

15. Capanema, E.A; Balakshin, M.Y.; Kadla, J.F. Quantitative characterization of a hardwood milled wood lignin by nuclear magnetic resonance spectroscopy. *J. Agric. Food. Chem.,* **2005**, *53*, 9639-9649.

16. Yuan, T.Q.; Sun, S.N.; Xu, F.; Sun, R.C. Structural characterization of lignin from triploid of *Populus tomentosa* Carr. *J. Agric. Food. Chem.*, **2011**, *59*, 6605-6615.

17. Abdulkhani, A.; Karimi, A.; Mirshokraie, A.; Hamzeh, Y.; Marlin, N.; Mortha, G. Isolation and chemical structure characterization of enzymatic lignin from *Populus deltoides* Wood. *J. Appl. Polym. Sci.*, **2010**, *118,* 469-479.

18. Younker, J.; Beste, A.; Buchanan, A. C., III. Computational study of bond dissociation enthalpies for lignin model compounds: beta-5 arylcoumaran. *Chem. Phys. Lett.* **2012**, *545,* 100−106.

19. Elder, T. Bond dissociation enthalpies of a dibenzodioxocin lignin model compound. *Energy Fuels* **2013,** *27*, 4785−4790.

20. Elder, T. Bond dissociation enthalpies of a pinoresinol lignin model compound. *Energy Fuels* **2014**, *28*, 1175−1182

21. Elder, Thomas; Berstis, Laura; Beckham, Gregg T.; Crowley, Michael. Coupling and Reactions of 5-Hydroxyconiferyl Alcohol in Lignin Formation. *J. Agric. Food. Chem.*, **2016**, *64*, 4742-4750.

22. Berstis, Laura; Elder, Thomas; Crowley, Michael; Beckham, G.T. The radical nature of C-lignin. *ACS Sustain. Chem. Eng.,* **2016**, *4*, 5327-5335.

23. Mar, B.D; Kulik, J. Depolymerization pathways for branching lignin spirodienone units revealed with *ab initio* steered molecular dynamics. *J. Phys. Chem. A* **2017**, *121*, 532-543.

24. Pople, J.A.; Head-Gordon, M.; Fox, D.J.; Raghavachari, K.; Curtiss, L.A. Gaussian-1 theory: A general procedure for prediction of molecular energies, *J. Chem. Phys.*, **1989**, *90*, 5622-5629.

25. Spartan'16, Wavefunction, Inc. Irvine, CA.

26. Gaussian 09, Revision E.01,M. J. Frisch, G. W. Trucks, H. B. Schlegel, G. E. Scuseria, M. A. Robb, J. R. Cheeseman, G. Scalmani, V. Barone, B. Mennucci, G. A. Petersson, H. Nakatsuji, M. Caricato, X. Li, H. P. Hratchian, A. F. Izmaylov, J. Bloino, G. Zheng, J. L. Sonnenberg, M. Hada, M. Ehara, K. Toyota, R. Fukuda, J. Hasegawa, M. Ishida, T. Nakajima, Y. Honda, O. Kitao, H. Nakai, T. Vreven, J. A. Montgomery, Jr., J. E. Peralta, F. Ogliaro, M. Bearpark, J. J. Heyd, E. Brothers, K. N. Kudin, V. N. Staroverov, T. Keith, R. Kobayashi, J. Normand, K. Raghavachari, A. Rendell, J. C. Burant, S. S. Iyengar, J. Tomasi, M. Cossi, N. Rega, J. M. Millam, M. Klene, J. E. Knox, J. B. Cross, V. Bakken, C. Adamo, J. Jaramillo, R. Gomperts, R. E. Stratmann, O. Yazyev, A. J. Austin, R. Cammi, C. Pomelli, J. W. Ochterski, R. L. Martin, K. Morokuma, V. G. Zakrzewski, G. A. Voth, P. Salvador, J. J. Dannenberg, S. Dapprich,

A. D. Daniels, O. Farkas, J. B. Foresman, J. V. Ortiz, J. Cioslowski, and D. J. Fox, Gaussian, Inc., Wallingford CT, 2013.

27. Gaussian 16, Revision A.03, M. J. Frisch, G. W. Trucks, H. B. Schlegel, G. E. Scuseria, M. A. Robb, J. R. Cheeseman, G. Scalmani, V. Barone, G. A. Petersson, H. Nakatsuji, X. Li, M. Caricato, A. V. Marenich, J. Bloino, B. G. Janesko, R. Gomperts, B. Mennucci, H. P. Hratchian, J. V. Ortiz, A. F. Izmaylov, J. L. Sonnenberg, D. Williams-Young, F. Ding, F. Lipparini, F. Egidi, J. Goings, B. Peng, A. Petrone, T. Henderson, D. Ranasinghe, V. G. Zakrzewski, J. Gao, N. Rega, G. Zheng, W. Liang, M. Hada, M. Ehara, K. Toyota, R. Fukuda, J. Hasegawa, M. Ishida, T. Nakajima, Y. Honda, O. Kitao, H. Nakai, T. Vreven, K. Throssell, J. A. Montgomery, Jr., J. E. Peralta, F. Ogliaro, M. J. Bearpark, J. J. Heyd, E. N. Brothers, K. N. Kudin, V. N. Staroverov, T. A. Keith, R. Kobayashi, J. Normand, K. Raghavachari, A. P. Rendell, J. C. Burant, S. S. Iyengar, J. Tomasi, M. Cossi, J. M. Millam, M. Klene, C. Adamo, R. Cammi, J. W. Ochterski, R. L. Martin, K. Morokuma, O. Farkas, J. B. Foresman, and D. J. Fox, Gaussian, Inc., Wallingford CT, 2016.

28. Foresman, J.B.; Frisch, A. *Exploring Chemistry with Electronic Structure Methods*, 3rd Edition. Gaussian, Inc., Wallingford, CT, 2015.

29. Zhao, Y.; Truhlar, D. G. Exploring the limit of accuracy of the global hybrid meta density functional for main-group thermochemistry, kinetics, and noncovalent interactions. *J. Chem. Theory Comput.* **2008**, *4*, 1849−1868.

30. Wheeler, S.E.; McNeil, A.C.; Müller, P.; Swager, T.M.; Houk, K.N. Probing substituent effects in aryl-aryl interactions using stereoselective diels-alder cycloadditions. *J. Am. Chem Soc.*, **2010**, *132*, 3304-3311.

31. Peverati R.; Truhlar D.G. Quest for a universal density functional: the accuracy of density functionals across a broad spectrum of databases in chemistry and physics. *Phil. Trans. R. Soc. A*, **2014**, *372*, 20120476.

32. Hohenstein, Edward G.; Chill, Samuel T.; Sherrill, C. David. Assessment of the Performance of the M05-2X and M06-2X Exchange-Correlation Functionals for Noncovalent Interactions in Biomolecules. *J. Chem. Theory Comput*. **2008**, *4*, 1996–2000.

33. Zhao, Y. and D.G. Truhlar. Applications and Validations of the Minnesota Density Functionals. *Chem. Phys. Lett*. **2011**, *502*, 1-13.

34. Wagner, Armin; Donaldson, Lloyd; Kim, Hoon; et al. Suppression of 4-Coumarate-CoA Ligase in the Coniferous Gymnosperm *Pinus radiata, Plant Physiol.*, **2009**, *149*, 370-383.

35. Stewart, Jaclyn J.; Akiyama, Takuya; Chapple, Clint; et al. The Effects on Lignin Structure of Overexpression of Ferulate 5-Hydroxylase in Hybrid Poplar. *Plant Physiol.*, **2009**, *150*, 621-635.